



# PRODUCTION OF CATHODE MATERIAL FOR OXYGEN ELECTRODES BY ANODIC OXIDIZATION OF MULTIWALL CARBON NANOTUBES

M.O. Danilov<sup>[a],\*</sup>, I.A. Rusetskii<sup>[a]</sup>, I.A. Slobodyanyuk<sup>[a]</sup>, O.Y. Khyzhun<sup>[b]</sup>,  
G.Ya. Kolbasov<sup>[a]</sup>

**Keywords:** Anodic oxidation of carbon nanotubes, Graphene oxide, Electrode materials, Oxygen electrode.

We report the synthesis of graphene oxide by the electrochemical method. The standard redox potentials of the carboxyl groups of carbon is used to select the oxidation potential. Graphene oxide obtained by anodic oxidation of multiwall carbon nanotubes in concentrated sulfuric acid, confirmed by electron microscopy, XRD, X-ray photoelectron spectroscopy, X-ray emission spectroscopy and Raman spectra, is a prospective electrode material for the chemical current sources. The oxidation potential in 96 % sulfuric acid is +3 V and the time of oxidation was 4 h. A good electrical conductivity is observed because of the presence of fragments of carbon nanotube in graphene oxide. Thus, this material is a very promising electrode material for oxygen electrodes. The current–voltage characteristics of the oxygen electrodes, based on electrochemically produced graphene oxide, is the graphene oxide produced by anodic oxidation of multiwall carbon nanotubes.

\*Corresponding Author:

E-Mail: danilovmickle@rambler.ru

[a] Vernadskii Institute of General and Inorganic Chemistry,  
National Academy of Science of Ukraine, 32–34 Palladin  
Avenue, 03680 Kyiv, Ukraine.

[b] Frantsevych Institute for Problems of Materials Science,  
National Academy of Sciences of Ukraine, 3 Krzhyzhanivsky  
Street, 03142 Kyiv, Ukraine.

temperature; unzipping by influence of a scanning tunneling microscope; electrochemical unrolling; the redox chemical synthesis. Among most technologically advanced methods, in our opinion, electrochemical process is paid much attention because it has the ability to control the process by changing three parameters: voltage, current, and time of this process.

## Introduction

Application of air or oxygen electrodes in devices generating electrical energy is useful; such application does cause environmental problems and allows to save nonrenewable natural resources. The air and oxygen electrode is a three-phase electrode–electrolyte–gas system, where the generation of electric current is localized at a phase boundary. The current magnitude generated at such gas diffusion electrode depends on the triple contact zone of these three phases. In its turn, the electrode itself is composed of catalyst and carrier. The interaction between them determines the quantity of generated current, which depends on catalyst being used. It is known that the most effective catalyst for oxygen recovery is platinum, which is a very expensive material. A great number of workers is forced to study other effective but less expensive catalysts.<sup>1</sup> Another problem is catalytically active and stable carrier. The benefits of carbon nanotubes used as the carrier are shown.<sup>2–4</sup> Presently, a series of studies have been reported using graphene as an electrode material for lithium-ionic accumulators<sup>5</sup> and also as a catalyst carrier for catalysts in fuel cells.<sup>6–10</sup>

At the moment the methods known for the synthesis of graphene from carbon nanotubes are:<sup>11</sup> intercalation of alkaline earth elements and nitrogen; plasma etching; microwave unzipping; unzipping by catalytic metal nanoparticles; ultrasonic unzipping; opening-up by laser irradiation; electrical unzipping; hydrogenating at the high-

Although extensive studies have been performed to obtain graphene nanosheets via electrochemical exfoliation of graphite,<sup>12</sup> Pillai and his group are unique who suggested that in aqueous electrolytes using electrochemical oxidizing and reducing, longitudinal splitting and unzipping single<sup>13</sup> and multiwall carbon nanotubes (MWNTs)<sup>14</sup> are possible to be synthesized. According to Pillai, inducing electric field at the phase boundary results in the cleavage of carbon-carbon, similar to the mechanism of oxidation of olefin to the diol,<sup>15,16</sup> by forming the complex manganese ester.<sup>17,18</sup> Further, the diol is oxidized to form keto groups and complete rupture of the C = C bonds. Experimental studies,<sup>19</sup> as well as results obtained by Tour and co-workers<sup>20–22</sup> have shown that the unzipping of MWCNTs is most likely due to the intercalation of oxidized molecules in the defects in multi-walled carbon nanotubes.

Formation of surface groups on highly oriented pyrolytic graphite (HOPG) by electrochemical oxidation and intercalation acid anions is described.<sup>23–27</sup> Electro oxidation mechanism was studied in sulfuric acid, and it shows the formation of alcohol and other functional groups on the basal plane of HOPG surface.<sup>25</sup> As a result of oxidation, the surface was hydrophilic for its nature.<sup>28</sup> This phenomenon has been useful for the dispersion of graphene oxide (GO) in deionized water.<sup>29</sup> The use of sulfuric acid leads to a strong oxidation of graphene surfaces to form thin sheets with a large number of the structure defects.<sup>30</sup> High resistivity of graphene oxide is due to defects caused by damages of  $sp^2$ -structure.<sup>31</sup>

Graphene is usually obtained as a mixture of mono-, bi- and multilayer (3 – 10 monolayers) structured irregular flakes or plane sheets.<sup>32</sup> Based on the standard redox potentials of carbon<sup>33</sup> (Table 1) the required oxidant potential in acidic medium should be higher than + 0.528 V.

**Table 1.** Oxidant potentials in acidic and alkaline mediums

Acidic, in V		Alkaline	
C,H <sup>+</sup> /CH <sub>3</sub> OH	−0.320	C/CH <sub>3</sub> OH,OH	−1.480
HCO <sub>2</sub> H,H <sup>+</sup> /C	+0.528	CHO <sub>2</sub> <sup>1−</sup> /C,OH <sup>−</sup>	−0.603
CO,H <sup>+</sup> /C	+0.518	CO <sub>3</sub> <sup>2−</sup> /C,OH <sup>−</sup>	−0.766
H <sub>2</sub> CO <sub>3</sub> ,H <sup>+</sup> /C	+0.207		

At the electrochemical oxidation of multi-walled carbon nanotube, electrode potential is more electropositive because of the polarization of the electrode-collector material, the ohmic losses in the MWCNT and kinetic difficulties. This is confirmed by experimental data on the oxidation of MWCNTs in sulfuric acid at potentials between 0.7 and 4.8 V relative to the silver-chloride electrode.<sup>34</sup> In a review,<sup>19</sup> numerous works on the anodic oxidation of different forms of carbon in sulfuric acid at electrodes of various materials at a voltage of 1 to 10 V are discussed. Based on analysis of existing literature data, the possibility of obtaining the graphene oxide by anodic oxidation of multi-walled carbon nanotubes, to the best of our knowledge, has not been attempted as yet.

Based on the above studies it is clear that there is no consensus on the possibility of obtaining the graphene oxide by anodic oxidation of multi-walled carbon nanotubes. Therefore, the aim of this study was to investigate the possibility of obtaining graphene oxide, using carbon nanotubes as a starting material, by simple technology method for the production of the electrode material for the oxygen electrodes of the fuel cells.

## Experimental

For the electrochemical production of graphene oxide, multi-walled carbon nanotubes were used. The outer diameter of MWCNTs was about 10 – 30 nm, the specific surface area was 230 m<sup>2</sup> g<sup>−1</sup>, with a bulk density of 25 – 35 g dm<sup>−3</sup>. The number of walls ranges from 8 to 15. Anodic oxidation of carbon nanotubes was conducted in a 150 ml glass beaker containing 96 % sulfuric acid solution, the weight of MWCNT was 1 g. The container for the oxidation of MWCNT is a bag that served as a membrane in lead accumulators, which is stable in acid, is used. For the firmly pressed MWCNTs to the anode electrodes, PTFE liners were used. Titanium and platinum electrodes are used as cathodes and the anodes respectively. Oxidation of carbon nanotubes was carried out in the galvanostatic mode. A silver-chloride electrode connected through a salt bridge was used as a reference electrode. The samples of graphene oxide (GO) obtained by the electrochemical oxidation of the

carbon nanotubes were examined with a JEM–100 CXII electron microscope. The X-ray phase analysis was performed using a DRON–4 X-ray diffractometer employing CuK<sub>α</sub> irradiation. Raman spectra of initial MWCNTs and GO were registered by INVIA Raman microscope (Renishaw) under the excitation of He-Ne laser with  $\lambda_{\text{ex}} = 0.6328 \text{ Å}$ . The position of standard Si sample at 520 cm<sup>−1</sup> was used as the reference for wavenumber calibration. WiRE 3.4 software was used for Raman data acquisition and data analysis. The presence of oxygen-containing groups in graphene oxide was analyzed employing the X-ray photoelectron spectroscopy (XPS) method. The XPS spectra of graphene oxide and, for comparison, pristine multiwall carbon nanotubes (MWCNTs) were recorded using the UHV-Analysis-System designed and assembled by SPECS Surface Nano Analysis Company (Berlin, Germany). The UHV-Analysis-System is supplied with a hemispherical PHOIBOS 150 analyzer. The XPS spectra of the graphene oxide and MWCNTs were recorded in an ion-pumped chamber at a base pressure less than  $8 \cdot 10^{-10}$  mbar. The XPS spectra of the above mentioned carbon materials were excited by a MgK<sub>α</sub> source of X-ray irradiation ( $E = 1253.6 \text{ eV}$ ) and were measured at a constant pass energy of 30 eV. Furthermore, the X-ray emission spectroscopy (XES) method is recognized as a very powerful technique when studying carbon materials<sup>35,36</sup> by measuring the XES CK<sub>α</sub> band, which represents the energy distribution of the C 2*p* states. Technique of recording the XES CK<sub>α</sub> band (K → L<sub>II,III</sub> transition) was similar to that described.<sup>37</sup> Briefly, the XES CK<sub>α</sub> bands of graphene oxide and MWCNTs were acquired employing an RSM–500 spectrometer-monochromator equipped with a diffraction grating (600 groves / mm, radius of curvature of  $R = 6026 \text{ mm}$ ). Secondary electron multiplier VEU–6 with a CsI photocathode was used as a detector. Working condition of a spectrometer electron gun when exciting the XES CK<sub>α</sub> bands was set as follows:  $U_a = 5.0 \text{ kV}$  and  $I_a = 2.2 \text{ mA}$ . Energy resolution of the RSM–500 spectrometer was evaluated to be 0.25 eV when measuring the XES CK<sub>α</sub> bands of graphene oxide and MWCNTs.

The synthesized materials were prepared by pressing two-layer oxygen electrodes. The hydrophobic layer contained 0.07 g / cm<sup>2</sup> acetylene black with 25 % polytetrafluoroethylene, and the active layer contained 0.02 g / cm<sup>2</sup> RGO, with 5 % polytetrafluoroethylene. The studies were carried out on a fuel cell mockup, a zinc electrode being used as the anode. A mockup for the testing of gas-diffusion electrodes is described.<sup>38</sup> The electrolyte was a 6 M KOH solution. A silver-chloride electrode connected through a salt bridge was used as a reference electrode. The electrochemical characteristics were recorded under galvanostatic conditions. The oxygen source was a U-shaped electrolyzer with alkaline electrolyte. Oxygen was supplied to the gas electrodes under an excess pressure of 0.01 MPa. Before measurements, the oxygen electrode was blown through with oxygen over an hour.

The characteristics of the oxygen electrode from the electrode materials obtained by the anodic oxidations of carbon nanotubes were compared with the characteristics of electrodes from the initial MWCNT with deposited platinum black. Platinum is deposited by electrochemical method from an aqueous solution containing 3 % H<sub>2</sub>PtCl<sub>6</sub> and 0.2 % lead acetate (II) at a voltage of 1 V for 2 min; the current direction is changed through 30 s.

## Results and Discussion

We investigated the dependence of the electrochemical characteristics of oxygen electrodes based on the GO obtained by the oxidation of MWCNTs with various time. Anodic oxidation of MWCNT was performed at a potential + 3 V over 1.5, 4, and 5 h. As can be seen from the current–voltage curves plotted for the oxygen electrode (Figure 1), increasing the anodic oxidation time to 4 hours leads to increase of the electrochemical characteristics of the electrodes (Curve 2). With further increase of the time of oxidation the characteristics do not vary significantly (Curve 3).

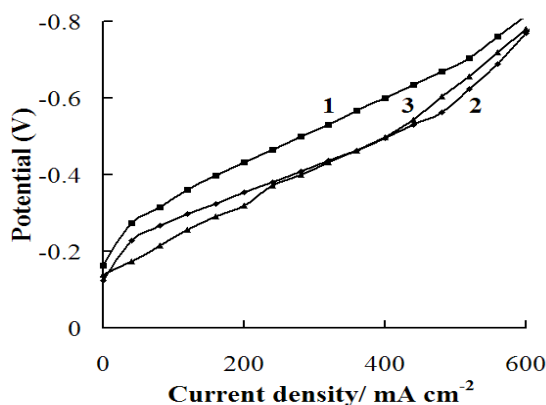


**Figure 1.** Dependence of potential on current density for oxygen electrodes with the active layer in an amount of 0.02 g / cm<sup>2</sup> consisting of graphene oxide prepared by electrochemical oxidation of MWCNTs at the potential + 3 V with different oxidation time: (1) 1.5, (2) 4 and (3) 5 h.

We have also carried out the oxidation of MWCNTs at the different potentials over 4 hours. Potential ranged from + 1.8 V to + 4.5 V. As shown in Figure 2, the anodic oxidation of multiwalled carbon nanotubes over 4 h at the potential of + 3.0 V produces the most catalytically active materials for oxygen electrode.

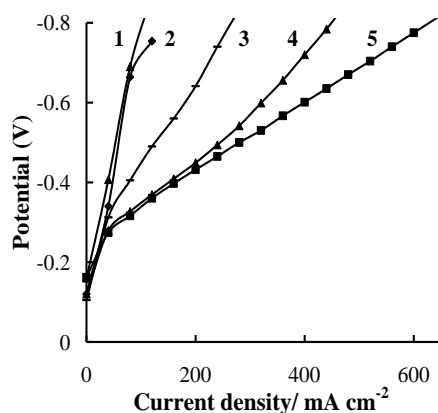


**Figure 2.** Dependence of potential on current density for oxygen electrodes with the active layer in an amount of 0.02 g / cm<sup>2</sup> consisting of the graphene oxide prepared by electrochemical oxidation of MWNTs at various potentials (V): (1) initial MWCNTs, (2) + 1.8, (3) + 4.5, (4) + 2.5, and (5) + 3.0 V.

Materials obtained by anodic oxidation of MWCNTs were investigated by means of various physical and chemical methods. Figure 3 shows the XRD analysis of the obtained samples.

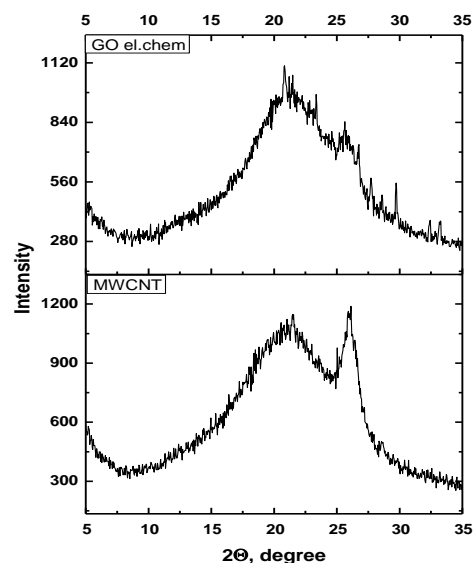


**Figure 3.** XRD patterns of the samples of initial MWCNTs (MWCNT, bottom panel) and graphene oxide (GO el.chem, upper panel) obtained by electrochemical oxidation of the multi-walled carbon nanotubes.

As one can see from the micrograph presented in Figure 4a, employing the anodic oxidation of carbon nanotubes, we have obtained samples of graphene oxide. Closely spaced tags of the carbon atoms in the diffraction ring, Figure 4b, show that the obtained sample consists of undulating planar multilayer's of graphene oxide. The case of obtaining such graphene is reported.<sup>32</sup> From micrographs, number of layers of graphene oxide was estimated that ranges from 3 to 10. Also, there are fragments of the original multi-walled carbon nanotubes into graphene oxide, which leads to good electrical conductivity of received materials, as opposed to pure graphene oxide. This is evidenced by good electrochemical characteristics of oxygen electrodes obtained in the present work based on graphene oxide (Figures 1 and 2). Figure 5 shows Raman spectra obtained at 633 nm and intensity of 50 % for the graphene oxide prepared by anodic oxidation of MWCNTs in the acidic medium. Analysis of Raman spectra confirms the presence of graphene oxide multilayers.

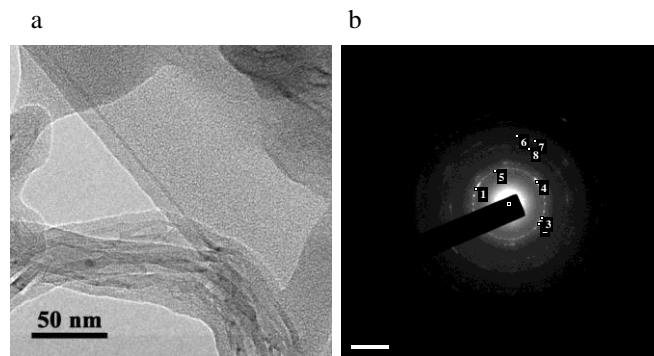


**Figure 4.** (a) Electron micrograph of graphene oxide obtained by anodic oxidation of MWCNTs, and (b) the diffraction of this sample

Figures 4a and b show an electron micrograph of graphene oxide obtained by electrochemical oxidation of carbon nanotubes and the diffraction of this sample, respectively.

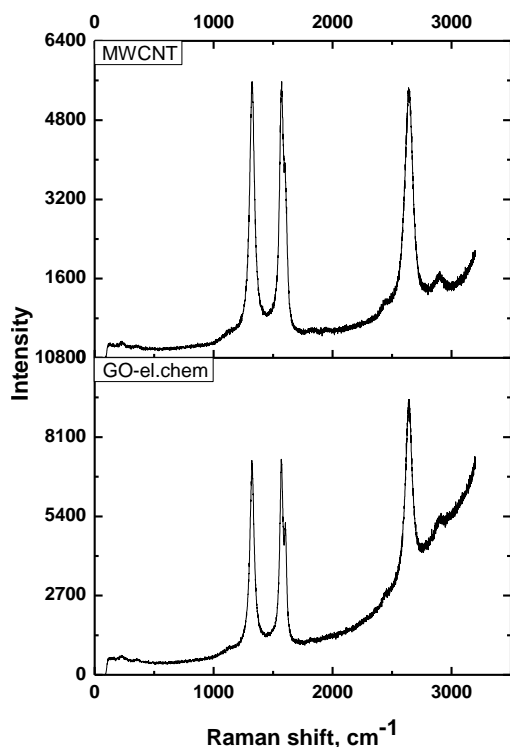
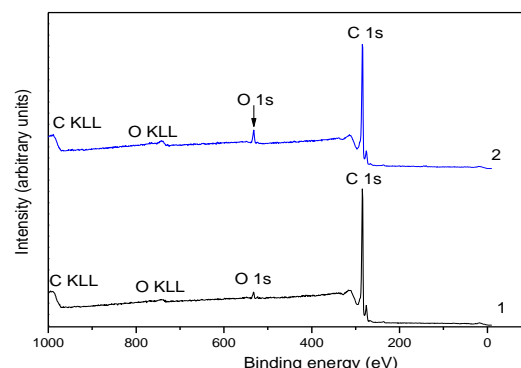


**Figure 5.** Raman spectra obtained at 633 nm and intensity of 50 % for graphene oxide (GO el.chem, bottom panel) obtained by anodic oxidation of MWNTs and initial MWCNTs (MWCNT, upper panel).

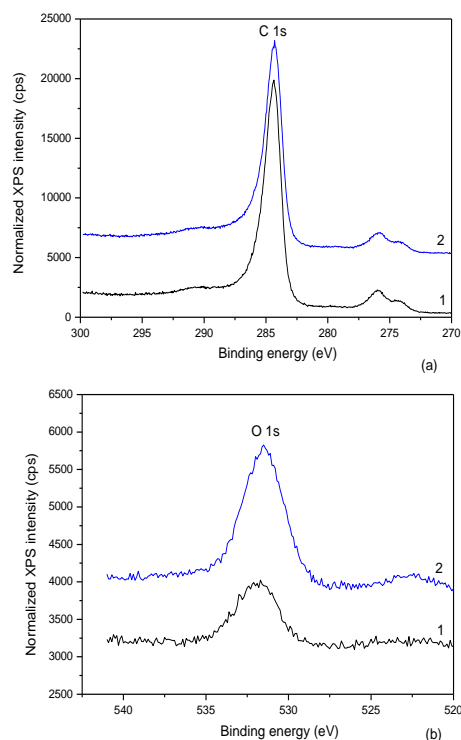
Figure 6 presents the XPS spectra of the graphene oxide and MWCNTs under study. Results of the present XPS measurements indicate that the surface of the pristine MWCNTs reveals the presence of oxygen, with the binding energy of the O 1s core level electrons that is equal to 531.9 eV. This binding energy value corresponds to oxygen-containing species adsorbed on the MWCNTs surface due to exposure of the specimen to air for a long time (several weeks). When going from MWCNTs to graphene oxide, the relative intensity of the XPS O 1s core-level spectrum increases (Figure 6) and its binding energy decreases by about 0.5 eV (Figure 7). The later effect can be explained by the fact that the XPS O 1s core-level spectrum of graphene oxide is a superposition of the spectra of oxygen belonging to adsorbed oxygen-containing species and of oxygen binding with graphene. The precise measurements of the XPS C 1s core-level spectra (Figure 7a) allow for concluding that the maxima of the spectra coincide within accuracy of the present measurements ( $\pm 0.05$  eV) for the both samples under study. Furthermore, it is worth mentioning that binding energies of the maxima of the XPS C 1s core-level spectra of the graphene oxide and MWCNTs, as it is evidenced from Figure 7a, are close to that of graphite, namely 284.4 eV.<sup>39</sup>

Figure 8 presents the XES CK $\alpha$  bands measured for graphene oxide and MWCNTs. It has been reported<sup>40,41</sup> that in the high-energy portion of the XES C K $\alpha$  band of MWSNTs the  $\pi$ - and  $\pi^+\sigma$ -binding states are positioned.

These states correspond to the fine-structure peculiarities labeled as “c”, “d”, “e” of the XES CK $\alpha$  band that are well resolved for the both samples under study (Figure 8). The mentioned states represent the energy distribution of the C<sup>2p</sup> states involved in the mixed  $pp\sigma^+$  /  $pp\pi$  and pure  $pp\pi$  interactions<sup>40</sup> in the radial planes and along the axis of



**Figure 6.** Survey XPS spectra of (1) MWCNTs and (2) graphene oxide.



**Figure 7.** Detailed XPS (a) C 1s and (b) O 1s core-levels spectra of (1) MWCNTs and (2) graphene oxide

MWCNTs, respectively.<sup>40,41</sup> It is worth indicating that the XES C K $\alpha$  band derived in the present work for MWCNTs, by its shape and energy positions of the fine-structure peculiarities, resembles the similar bands recorded in Ref.<sup>41</sup> for 200-walled nanotubes with a diameter of 140 nm and double-walled nanotubes with a diameter of 4 nm obtained in arc discharge without catalysts by MER-corporation. In the latter work, it has been established that the bandwidth of the CK $\alpha$  band of double-walled carbon nanotubes reduces in comparison with that of the 200-walled carbon nanotubes only near the band maximum (at  $I > 0.75 I_{\max}$ ).



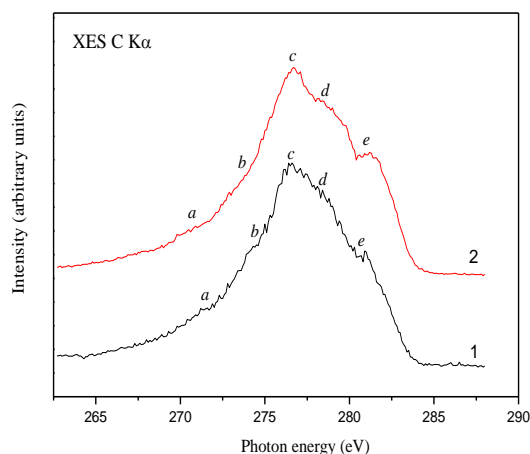


**Figure 8.** The XES  $CK\alpha$  bands of (1) MWCNTs and (2) graphene oxide.

This effect is explained in Ref.<sup>41</sup> as a result of a decrease of the  $\pi^+\sigma$ -overlapping in the radial plane inside the 200-walled carbon nanotubes with an increase in diameter of every following wall. As a consequence, the C  $2p$  states involved in such bonds shift toward higher photon energies.<sup>41</sup>

As can be seen from Figure 8, when going from MWCNTs to graphene oxide synthesized in the present work, visible changes occur in the shape of the XES  $CK\alpha$  band. In particular, the sub-band “e” of the XES  $CK\alpha$  band appearing due to the existence of the C  $2p$  states involved in pure  $pp\pi$  interactions increases its width in graphene oxide. Furthermore, the maximum “c” of the XES  $CK\alpha$  band, where mixed  $pp\sigma^+ / pp\pi$  interactions are located, becomes narrower when going from MWCNTs to graphene oxide.

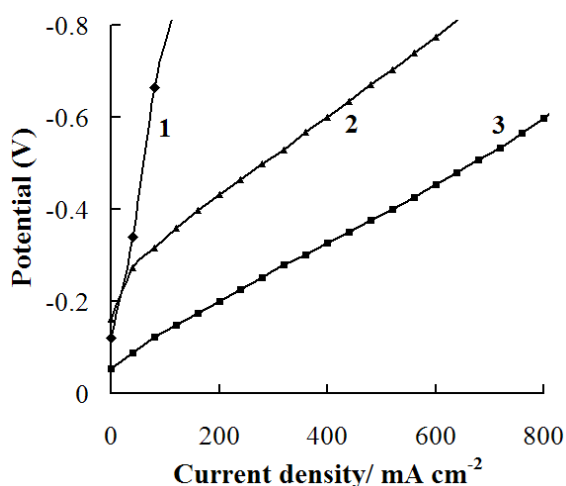


**Figure 9.** Dependence of potential on current density for oxygen electrodes with the active layer in an amount of  $0.02 \text{ g / cm}^2$  consisting of: (1) initial MWCNTs; (2) graphene oxide produced by oxidation of MWCNTs in sulfuric acid for 4 h at an anode potential of +3.0; (3) MWCNTs with deposited platinum in an amount of 10 wt. %.

Figure 9 shows the comparative characteristics of the oxygen electrodes on the basis of initial MWCNTs (Curve 1), graphene oxide obtained by electrochemical oxidation of MWCNTs (Curve 2) and MWCNTs with deposited platinum (curve 3). As one can see from Figure 9, the electrocatalytic characteristics of electrodes based on graphene oxide are close to the characteristics of electrodes based on platinum-containing materials. All examined graphene oxide materials were stable within six months when being tested in the galvanostatic regime in the fuel-element mockup at a current density of  $200 \text{ mA / cm}^2$  at oxygen electrodes.

Based on these results, we can conclude that using anodic electrochemical oxidation of multi-walled carbon nanotubes over 4 h in electrolyte of 96 % sulfuric acid at a potential of +3 V, graphene oxide can be synthesized.

## Conclusion

Graphene oxide was synthesized in the present work by anodic oxidation of multi-walled carbon nanotubes. We have determined that the most appropriate conditions for such a synthesis are as follows: oxidation potential in 96 % sulfuric acid is +3 V and the oxidation duration is 4 h. The formation of well defined graphene oxide was confirmed by data of electron microscopy, X-ray diffraction, X-ray photoelectron spectroscopy, X-ray emission spectroscopy and Raman spectra. In particular, comparative XPS studies of graphene oxide and MWCNTs indicate that the surface of pristine MWCNTs reveals the presence of oxygen, with the binding energy that corresponds to oxygen-containing species adsorbed on the MWCNTs surface due to exposure of the specimen to air for a long time (several weeks). Our XPS data reveal that when going from MWCNTs to graphene oxide, the XPS O  $1s$  core-level binding energy decreases by about 0.5 eV that can be explained by the fact that the XPS O  $1s$  spectrum of graphene oxide is a superposition of the spectra of oxygen belonging to adsorbed oxygen-containing species and of oxygen binding with graphene. The maxima of the XPS C  $1s$  core-level spectra coincide within accuracy of the present measurements ( $\pm 0.05 \text{ eV}$ ) for graphene oxide and MWCNTs under study. However, when going from MWCNTs to graphene oxide, visible changes occur in the shape of the XES  $CK\alpha$  band, representing the energy distribution of the C  $2p$  states. In particular, the high-energy sub-band appearing due to the existence of the C  $2p$  states involved in pure  $pp\pi$  interactions increases its width in graphene oxide, while the main maximum of the XES  $CK\alpha$  band, where mixed  $pp\sigma^+ / pp\pi$  states are located, becomes narrower when going from MWCNTs to graphene oxide. Furthermore, due to the presence of fragments of carbon nanotubes in graphene oxide synthesized, the latter reveals good electrical conductivity. Therefore, this material is expected to be a very promising electrode material for oxygen electrodes of power sources.

## Acknowledgement

This paper has been presented at the 4th International Conference “Nanotechnologies”, October 24 – 27, 2016, Tbilisi, Georgia (Nano – 2016).

## References

- <sup>1</sup>Bidault, F., Brett, D. J. L., Middleton, P. H., Brandon, N. P., *J. Power Sources*, **2009**, 187, 39.
- <sup>2</sup>Soehn, M., Lebert, M., Wirth, T., Hofmann, S., Nicoloso, N., *J. Power Sources*, **2008**, 176, 494.
- <sup>3</sup>Hsieh, C.-T., Lin, J.-Yi., Wei, J.-L., *Int. J. Hydrogen Energy*, **2009**, 34, 685.
- <sup>4</sup>Wang, X., Waje, M., Yan, Y., *Electrochem. Solid-State Lett.*, **2005**, 8, A42.
- <sup>5</sup>Wang, G., Shen, X., Yao, J., Park, J., *Carbon*, **2009**, 47, 2049.
- <sup>6</sup>Xin, Y., Liu, J., Jie, X., Liu, W., Liu, F., Yin, Y., Gu, J., Zou, Z., *Electrochim. Acta*, **2012**, 60, 354.
- <sup>7</sup>Lin, Z., Waller, G., Liu, Y., Liu, M., Wong, C. P., *Adv. Energy Mater.*, **2012**, 2, 884.
- <sup>8</sup>Qu, L. T., Liu, Y., Baek, J. B., Dai, L. M., *ACS Nano*, **2010**, 4, 1321.
- <sup>9</sup>Lin, Z. Y., Song, M. K., Ding, Y., Liu, Y., Liu, M. L., Wong, C. P., *Phys. Chem. Chem. Phys.*, **2012**, 14, 3381.
- <sup>10</sup>Shao, Y., Zhang, S., Wang, C., Nie, Z., Liu, J., Wang, Y., Lin, Y., *J. Power Sources*, **2010**, 195, 4600.
- <sup>11</sup>Danilov, M. O., Slobodyanyuk, I. A., Rusetskii, I. A., Kolbasov, G. Ya., in: Aliofkhazraei, M., Ali, N., Milne, W. I., Ozkan, C. S., Mitura, S., Gervasoni J. L. (Eds.), *Graphene Science Handbook. Fabrication Methods*, CRC Press/Taylor & Francis, **2016**, 205.
- <sup>12</sup>Low, C. T. J., Walsh, F. C., Chakrabarti, M. H., Hashim, M. A., Hussain, M. A., *Carbon*, **2013**, 54, 1.
- <sup>13</sup>John, R., Shinde, D. B., Liu, L., Ding, F., Xu, Z., Vijayan, C., Pillai, V. K., Pradeep, T., *ACS Nano*, **2014**, 8, 234.
- <sup>14</sup>Shinde, D. B., Debgupta, J., Kushwaha, A., Aslam, M., Pillai, V. K., *J. Am. Chem. Soc.*, **2011**, 133, 4168.
- <sup>15</sup>Waters, W. A., *Quart. Rev. Chem. Soc.*, **1958**, 12, 277.
- <sup>16</sup>Ohloff, G., Giersch, W., *Angew. Chem., Int. Ed. Engl.*, **1973**, 12, 401.
- <sup>17</sup>Kosynkin, D. V., Higginbotham, A. L., Sinitskii, A., Lomeda, J. R., Dimiev, A., Price, B. K., Tour, J. M., *Nature*, **2009**, 458, 872.
- <sup>18</sup>Higginbotham, A. L., Kosynkin, D. V., Sinitskii, A., Sun, Z., Tour, J. M., *ACS Nano*, **2010**, 4, 2059.
- <sup>19</sup>Low, C. T. J., Walsh, F. C., Chakrabarti, M. H., Hashim, M. A., Hussain, M. A., *Carbon*, **2013**, 54, 1.
- <sup>20</sup>Dimiev, A. M., Tour, J. M., *ACS Nano*, **2014**, 8, 3060.
- <sup>21</sup>James, D. K., Tour, J. M., *Acc. Chem. Res.*, **2013**, 46, 2307.
- <sup>22</sup>James, D. K., Tour, J. M., *Macromol. Chem. Phys.*, **2012**, 213, 1033.
- <sup>23</sup>Hathcock, K. W., Brumfield, J. C., Goss, C. A., Irene, E. A., Murray, R. W., *Anal. Chem.*, **1995**, 67, 2201.
- <sup>24</sup>Skowronski, J. M., *Synth. Metal.*, **1995**, 73, 21.
- <sup>25</sup>Bourelle, E., Claude-Montigny, B., Metrot, A., *Mol. Cryst. Liq. Cryst.*, **1998**, 310, 321.
- <sup>26</sup>Alliata, D., Haring, P., Haas, O., Kotz, R., Siegenthaler, H., *Electrochem. Commun.*, **1999**, 1, 5.
- <sup>27</sup>Schnyder, B., Alliata, D., Kotz, R., Siegenthaler, H., *Appl. Surface Sci.*, **2001**, 173, 221.
- <sup>28</sup>Choo, H. S., Kinumoto, T., Jeong, S. K., Iriyama, Y., Abe, T., Ogumi, Z., *J. Electrochem. Soc.*, **2007**, 154, B1017.
- <sup>29</sup>Dilimon, V. S., Sampath, S., *Thin Solid Films*, **2011**, 519, 2323.
- <sup>30</sup>Su, C. Y., Lu, A. Y., Xu, Y., Chen, F. R., Khlobystov, A. N., Li, L. J., *ACS Nano*, **2011**, 5, 2332.
- <sup>31</sup>You, X., Chang, J. H., Ju, B. K., Pak, J. J., *J. Nanosci. Nanotechnol.*, **2011**, 11, 5965.
- <sup>32</sup>Yan, L., Zheng, Y. B., Zhao, F., Li, S., Gao, X., Xu, B., Weiss, P. S., Zhao, Y., *Chem. Soc. Rev.*, **2012**, 41, 97.
- <sup>33</sup>Bratsch, S. G., *J. Phys. Chem.*, **1989**, 18, 1.
- <sup>34</sup>Zehtab, A. Y., Roberts, E. P. L., Sundararaj, U., *Mat. Research Bull.*, **2016**, 80, 243.
- <sup>35</sup>Meisel, A., Leonhardt, G., Szargan, R., *X-Ray Spectra and Chemical Binding*, Springer-Verlag, Berlin/Heidelberg, **1989**.
- <sup>36</sup>Kurdyumov, A. V., Britun, V. F., Khyzhun, O. Y., Zaulychnyy, Y. V., Bekenev, V. L., Dymarchuk, V. O., Danilenko, A. I., *Diamond Relat. Mater.*, **2011**, 20, 974.
- <sup>37</sup>Khyzhun, O. Y., Zhurakovsky, E. A., Sinelnichenko, A. K., Kolyagin, V. A., *J. Electron Spectrosc. Relat. Phenom.*, **1996**, 82, 179.
- <sup>38</sup>Danilov, M. O., Kolbasov, G. Ya., Rusetskii, I. A., Slobodyanyuk, I. A., *Russ. J. Appl. Chem.*, **2012**, 85, 1536.
- <sup>39</sup>Khyzhun, O. Y., *J. Alloys Compd.*, **1997**, 259, 47.
- <sup>40</sup>Östling, D., Tománek, D., Rosén, A., *Phys. Rev. B*, **1997**, 55, 13980.
- <sup>41</sup>Zaulychnyy, Y. V., Solonin, Y. M., Foya, O. O., Khyzhun, O. Y., Vasylykiv, O., *Metallofiz. Noveishie Tekhnol.*, **2008**, 30, 169.

Received: 27.11.2016.

Accepted: 06.01.2017.